GANIL

GRAND ACCÉLÉRATEUR NATIONAL D'IONS LOURDS - CAEN
LABORATOIRE COMMUN IN2P3 (CNRS) - D.S.M. (CEA)

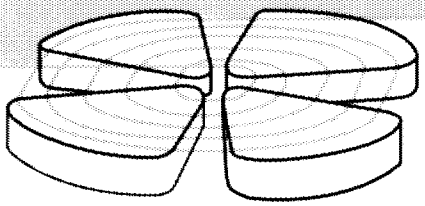

From RIB production to the applications for accelerator driven hybrid systems[a]

D. Ridikas and W. Mittig

Grand Accélérateur National d'Ions Lourds (GANIL)
BP 5027, F-14076 Caen Cedex 5, France

GANIL P 99 12

APH N.S., Heavy Ion Physics ? (1999) 00?-00?

HEAVY ION PHYSICS
©Akadémiai Kiadó

From RIB production to the applications for accelerator driven hybrid systems[a]

D. Ridikas and W. Mittig

Grand Accélérateur National d'Ions Lourds (GANIL)
BP 5027, F-14076 Caen Cedex 5, France

Received 22 March 1999

Abstract. The revival of interest for production of neutrons by light projectiles has been recently renewed because they are the basis in the development of powerful neutron sources for various applications like nuclear energy production and incineration of nuclear waste, material structure analysis, tritium production, etc. Another interest is related to the possibility of the production of radioactive ion beams (RIB) by neutron induced fission. One of the most important tasks in this context is to determine the most efficient way to convert the primary beam energy into neutrons produced afterwards. The problem is investigated by varying the incident energy of different projectiles for different target materials and assemblies. Consequently, a few direct applications of our investigations are presented and compared with experimental data or other theoretical estimations.

[a] At the request of the editor.

1. Introduction

When an energetic particle hits the target material consisting of heavy nuclei, tens of neutrons might be generated. In nuclear physics this process is known from the 1950s [1] and called a spallation reaction. Taking advantage of the progress in accelerator technologies in recent years the old idea of an intense neutron generator has revived to be exploited in many domains like solid state and material structure analysis, for which a continuous neutron source is being built at PSI (SINQ) [2], a high-flux pulsed source is in project at the European level (ESS project) [3] as well as in the US (SNS project) [4]. Intense neutron flux may also be used to produce isotopes for medicine or tritium production (APT project, US) [5]. The application that has been dominant driving force for the recent revival of the neutron production is the transmutation of radioactive waste and/or plutonium and nuclear

0231-4428/97/ $ 5.00

energy generation in subcritical spallation-fission hybrid reactors [6].

So far only medium energy (0.8 – 1.6 GeV) protons hitting a heavy target (U, Th, Pb) were considered as far as hybrid systems are concerned [7–10]. The use of projectiles such as deuterons and light targets (Li, Be) as converters to create the neutrons may have competitive, if not more efficient, features too [11]. This possibility was noticed by E.O. Lawrence already in 1947 after the very first experiments at the newly installed 184 inches cyclotron at Berkeley. Amusingly enough, it was also very early recognized that spallation reactions could be used for producing ^{239}Pu from depleted uranium and as an external source for neutrons for fission reactors (nearly the concept of the energy amplifier!) [12].

Another interest in the neutron production is related to the possibility of the production of Radioactive Ion Beams (RIB) by neutron induced fission [13–15]. Together with an increase in the accelerator power available, the new RIB targets will have to be designed to deal with high power densities. This is a problem of concern to a number of RIB facility concepts currently under consideration at various laboratories world wide. One effective solution to this problem, as initially proposed by the Argonne National Laboratory group [14], is to decouple the heat dissipation issue from that of nuclide production and release to the ion source. This can be achieved by stopping primary beam in a target-converter to produce an intense flux of neutrons to irradiate a secondary production target located behind the first one [14, 15].

One of the crucial problems, both for hybrid reactors and RIB production via neutron induced fissions, is to determine the most efficient way to convert the primary beam energy into neutrons produced afterwards. In this report we present and compare the predictions of neutron production induced by light projectiles, namely p, d and α, with the use of the existing Monte Carlo codes briefly presented in Chapter 1. We consider the incident energy of the projectiles, total neutron production, angular and energy distributions of emitted neutrons from different target materials and their further multiplication in the multiplying medium as the most important parameters of our interest (Chapter 2). Chapter 3 summarises already existing or plannned RIB production techniques. A combined RIB target assembly is proposed and model-based predictions of isotope production are made within the SPIRAL Phasé-II project at GANIL [15]. In Chapter 4 the energy gain in a simplified subcritical target assembly is estimated as a function of different incident projectiles as well as of different spallation target combinations. Our predictions are compared to available experimental data and other theoretical investigations.

2. The simulation codes

2.1. The LAHET Code System (LCS)

The LAHET Code System (LCS) [16] is a Monte Carlo code for the transport and interaction of nucleons, pions, muons, light ions ($Z \leq 4$), and antinucleons in complex geometries; it may also be used without particle transport to generate

particle production cross sections. For neutron energies $E_n \leq 20$ MeV the neutron transport down to thermal energies is performed using HMCNP, a modification of the MCNP code [17], which utilizes ENDF/B-VI based neutron cross section libraries. LAHET uses the same geometry system as MCNP.

In brief, the LAHET code [16] employs conventional intranuclear cascade (INC) and evaporation models (EVAP), and also contains the multistage preequilibrium exciton model (MPM). It has the capability of treating nucleus-nucleus interactions as well as particle-nucleus interactions. LAHET includes two different models of fission induced by high energy interactions. The Fermi breakup model has replaced the evaporation model for the disintegration of light nuclei ($A \leq 17$). We refer the reader to Ref. [16] where the physical models are explained in more detail and the results from running the LCS have been compared extensively against experimental data in a multitude of varying target materials, projectile type and energy, and geometry.

The recent International Code Comparison for Intermediate Energy Nuclear Data organized by NEA/OECD in Paris [18] have shown that the LCS generally has good/better predictive powers for spallation reactions if compared to other available models. However, we have to note that a characteristic narrow peak at large energies for emitted nucleons (almost the incident energy), which is well seen at forward angles, and which fades out with increasing scattering angle, is not properly reproduced for direct deuteron breakup on heavy metal targets ($Z \geq 26$). Following the estimations in [19], the missing part of this process, namely an elastic Coulomb breakup of deuteron, may contribute between 7% (in the case of neutrons) and 34% (in the case of protons) to the corresonding total nucleon production cross section calculated using the LCS, and it becomes less important for lighter targets.

2.2. CINDER'90 Codes and Data

CINDER'90 is a transmutation inventory code having a library of 63-group cross sections and requiring no library preparation prior to execution [20]. In conjunction with other codes simulating the radiation environment, CINDER'90 has been used to describe nuclide inventories in a variety of applications. CINDER'90 employs Markovian chains to determine temporal densities of nuclides in a radiation environment, solving independent contributions to atom densities in each of a number of linear nuclide chains. Nuclide concentrations are then obtained by summing partial concentrations (see [20] for more detailed description).

The library of nuclear data, constantly growing in breadth and quality, now describes 3400 nuclides in the range $1 \leq Z \leq 103$. CINDER'90 uses these data, e.g. ENDF/B-VI, Joint European Data File (JEF-1), European Activation File (EAF-3), Master Decay Library (MDL), etc. [20], and requires as input the description of the particle flux and the production probabilities of nuclides for reactions outside the particle and energy domain defined by the libraries. This is compatible with the LCS [16], which yields the medium-energy light projectile induced spallation products. These, together with the associated lower-energy neutron flux ($E_n \leq 20$ MeV)

from a companion calculation with HMCNP [17], may be employed by CINDER'90 afterwards for a final calculation.

3. Neutron production

3.1. Total neutron yield

A deuteron, already carrying one neutron, seems to be more efficient for neutron production than a proton. Consequently, an α-particle, with two neutrons and two protons, would be more favourable in the same context. As a matter of fact, the situation is more complicated. In Fig. 1 we present calculated total neutron yield

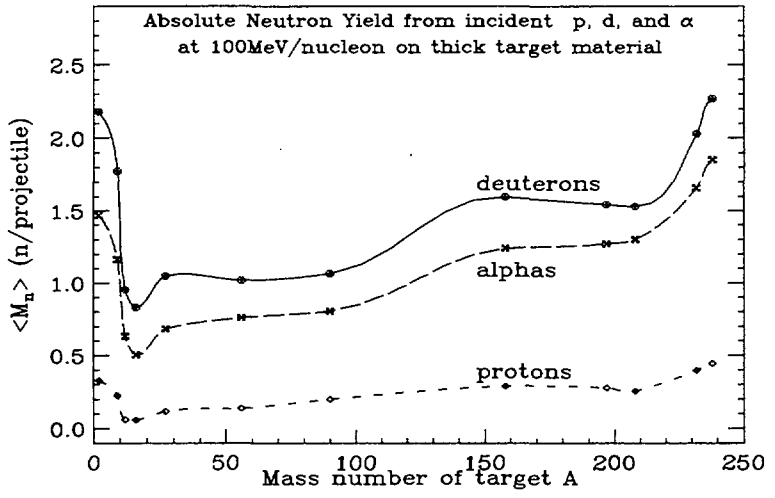

Fig. 1. Calculated neutron yield as a function of a thick (5 stopping ranges for deuterons) target material A for p, d and α-particles at 100 MeV per nucleon.

normalised per incident particle for protons, deuterons and α-particles at the incident energy of 100MeV per nucleon on different target materials. When the nucleus is bombarded with 200MeV deuterons, or 400MeV α-particles, the binding energy of the incident nucleons is important chiefly in causing a spatial correlation between them, and what happens can be thought of in terms of a simultaneous bombardment by several individual nucleons. Their characteristics depend primarily on the fact that the deuteron is a very loosely bound system. Contrary, an α-particle is more bound by one order of magnitude if compared to deuteron. It is also clear that neutron production by protons in this picture is very low as long as all incident particles have the same energy per nucleon.

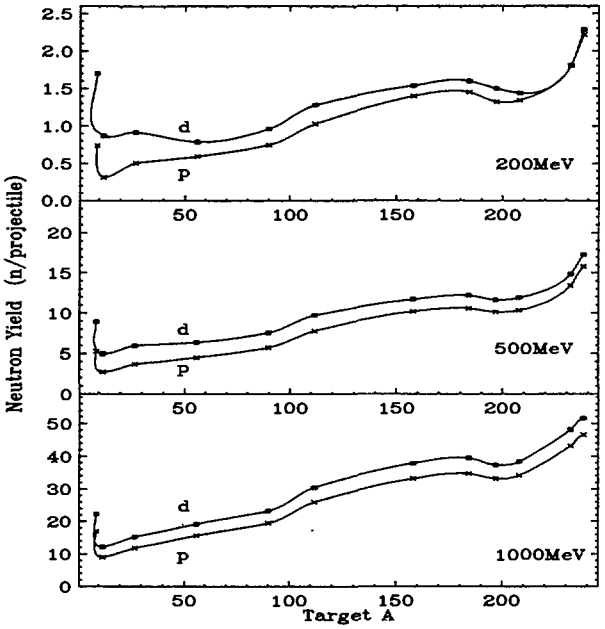

Fig. 2. Estimate of neutron production by protons (p) and deuterons (d) with total incident energies of 200MeV, 500MeV and 1000MeV. A thick target is a cylinder with equal length and diameter given by 2 stopping ranges for protons.

Since the total energy is one of the most essential parameters which defines the actual costs of particle acceleration, it is preferred to compare neutron production by protons and deuterons at the same total incident energies. It was estimated [11] that deuterons are more efficient projectiles for neutron production for all target materials if compared to protons, while α-particle induced reactions are least efficient at the same total incident energies. There is a simple explanation of that; neutron production will increase with a number of interactions, and this increases with the range $R \sim \frac{E^2}{M Z^2}$ following the energy loss relation. For a given energy E this favours protons with minimum $MZ^2=1$. However, an extra neutron very loosely bound in the projectile and the corresponding contribution from (n,xn) and (n,f) reactions easily compensates this effect for deuterons.

Fig. 2 represents total neutron yield from proton and deuteron induced reactions as a function of three incident energies and a number of thick target materials. It is clearly seen that the target dependence of the neutron yield is quite similar for both projectiles: the neutron production is more favourable for very light (Li or Be) and very heavy (Th or U) target materials. In the case of fissionable nuclei, the neutron production is increased further because of the contribution from fissions. For all

energies deuterons are much more efficient than protons in neutron production if one chooses very light targets. In the case of Be, neutron yield is higher for deuterons by a factor of 1.3-2.5 depending on energy as shown in Fig. 2. However, that is not the case for heavy targets. Here at 200MeV neutron production by protons and deuterons is almost the same. Increase in projectile energy makes deuterons more efficient only by 10% for U, for example, if compared to protons. It is also very important to notice that the neutron yield from light targets is comparable to the one from heavy targets only by deuteron induced reactions, while protons always produce considerably more neutrons on heavy targets than on the light ones (see the upper part of Fig. 2).

3.2. Angular and energy distributions of neutrons

By comparing the angular distributions for neutron production by protons and deuterons in our previous work we have shown [11] that in the case of protons, the angular distributions are relatively flat, while for deuteron induced reactions the neutron production is more concentrated at forward angles. On the other hand, both (p,xn) and (d,xn) reactions showed a some-what similar angular dependence at more backward angles; the cross section decreases considerably with the angle in the case of light and intermediate mass targets, while, in the case of the heavy ones, neutrons are emitted in the entire scattering angle range.

The energy distributions of neutrons emitted from (d,xn) and (p,xn) are quite different as well, i.e. much more energetic neutrons are produced by light targets than by heavy ones [11]. For example with projectiles of 200MeV, most of the neutrons (up to 80%) from U fall into the energy interval from 0 to 5MeV, while more than 50% of neutrons from Be are emitted with energies higher than 10MeV. Moreover, deuterons (comparing to protons) both in light target and heavy target materials produce considerably more energetic neutrons in absolute value. We refer the reader to Ref. [11] for more detailed discussion.

These observed differences might be very important in further investigations on neutron production within subcritical hybrid systems or RIB production assemblies, where the use of light or heavy metal targets, in our opinion, is still an open question. One could think of the combined system, for example, with a light target as a converter in order to create the neutrons (to be emitted at forward angles for light targets) and a heavy target (placed right after the light target) to increase the neutron flux further [21]. In this context (d,xn) reaction is much more favourable for two well established reasons. First of all, neutron production in absolute value is higher for light targets if one uses deuterons as we have shown above. Secondly, the neutrons created by deuterons in a light target are more forward peaked if compared to proton induced reaction; so these neutrons might be used more efficiently for secondary neutron production in a heavy target in terms of higher production rates and simpler geometry assemblies.

4. RIB production

4.1. Direct RIB production techniques

A significant increase of the intensities of RIBs would certainly open an access to the new domains of physics. One may consider that it will be possible to use beams of several MW, i.e. 3 orders of magnitude higher than currently used or scheduled at different RIB facilities world wide (presently all below the 10kW power limit) [22]. This would lead to the access of the reaction cross sections from the level of 10mb down to the μb level. The R&D programmes to develop high-intensity beams

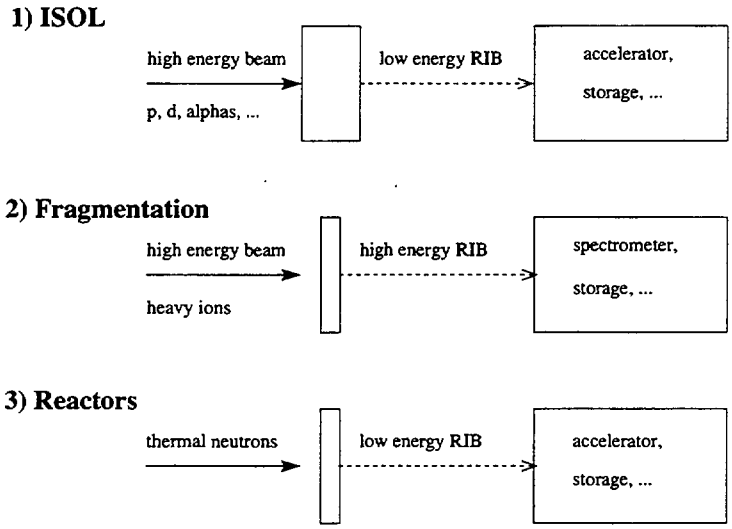

Fig. 3. Direct methods for the production of RIBs. From [22].

of a few MW are in progress, and in part stimulated by the projects related to the hybrid reactors, etc. Unfortunately, an increase of the primary beam intensity does not necessarily increases the intensity of the secondary RIBs, as was demonstrated in [23]. The authors argue that the maximum yield will be obtained for a limited power, and that there might be quite severe limitations with respect to the admissible power on a target [23].

Fig. 3 illustrates different direct methods to produce secondary beams. The first is the ISOL method (Isotope Separation On Line), pioneered by CERN-Isolde. As already discussed, it seems difficult to go much above the 10kW limit power deposited in the target. The highest maximum value was obtained (~20kW) and tested thermally by heating for the RIST target [23]. The second method is the

production of nuclei far from stability by high-energy fragmentation of heavy ion beams as pioneered by LBNL, and extensively used with high-intensity beams at GANIL, RIKEN, MSU and GSI. It is worth mentioning that these facilities devote more than half of their beam time to RIB physics. The highest power densities on target were obtained at GANIL with up to 1kW [22], and it seems to be no fundamental problems to produce beams of a few hundred kW with a bigger focus of the beam and a fast rotating target. However, in this particular case, the main limitations will be the maximum beam power of the accelerators already in use, and eventually radioprotection problems. The third method is based on thermal-neutron-induced fission, as in the PIAFE project [13]. Here the power limitations will be more or less the same as in the first case, in even more difficult environment, namely the source being situated near the centre of a high flux reactor. Nevertheless, at the upper limit (10kW) it would correspond to $3{\cdot}10^{14}$ fissions s^{-1}. In the

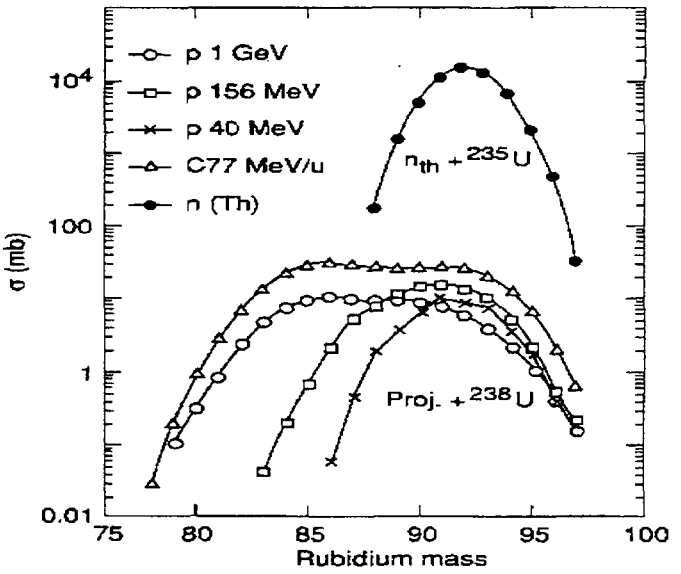

Fig. 4. Cross sections for production of Rb isotopes by various nuclear reactions. From [24].

most favourable range of the branching ratios of 1% and the transport efficiency of isotopes from the inside reactor to the external accelerator, say of the order of 1%, this would lead to the RIB intensities of $3{\cdot}10^{10}$ particles s^{-1} so far unreached.

Fig. 4 serves as an illustrative example of the production cross section of Rb isotopes by the three different RIB production techniques presented above, i.e. by fission of ^{238}U with protons of various energies, 77MeV per nucleon ^{12}C ions, and

thermal neutron fission of ^{235}U [24]. It is seen that the highest cross sections are found in the thermal fission of uranium, followed by heavy ion reactions which are somewhat higher that for the corresponding proton reactions. It should be noted, however, that the cross sections alone are insufficient to decide on the best suited reaction for production of RIBs, although it is always a good starting point. For a more realistic comparison of the different methods, it is important to take into account the final efficiency of the particular ion-source, that may reduce considerably, say 1-3 orders of magnitude, the final RIB intensity. The primary beam intensity is another essential parameter in this context as will be discussed below.

4.2. Combined methods: the case study for SPIRAL Phase-II

The considerations in the previous subsection suggest that it might be promising to look for more complex methods, with the main aim to decouple the heat and/or radioactivity produced by the primary beam from the ion source that produces the RIB. We refer the reader to the Ref. [22] where a few of these methods are mentioned with expected primary beam powers higher than 100kW. Below we present the case study of a particular combined RIB production assembly as initially proposed by the ANL group [14] and presently in the consideration as a future extension of the beams furnished by SPIRAL at GANIL (SPIRAL-2 hereafter) [15].

The highest fission yields can be obtained from uranium fission reactions. If thermal, reactor, and 14MeV neutron induced fissions are compared [25], it is suggested that more energetic neutrons give higher fission yields on the neutron-rich/deficient sides by a factor of 10-100. Therefore, with an increase in neutron energy one simply would expect even higher fission yields of the neutron-rich isotopes of interest. Different conclusions have been recently made in [26], where the thin target yields of neutron-rich fission products were estimated for a range of neutron energies from a few MeV up to 100MeV. The authors suggest that the best yields of neutron-rich isotopes of elements such as Kr, Rb, Xe and Cs are from 2-20MeV neutron induced fission of ^{238}U [26]. It was also concluded that high energy beams of neutrons have comparable integral yields per element, but the distributions are peaked at lower neutron numbers. This is presumably due to a higher neutron evaporation in the pre-equilibrium stage and/or the compound neucleus/fission stage.

On the other hand, in the combined target system, higher incident energies are preferred in order to produce considerably more neutrons in the primary target. As it will be shown below, a number of neutrons which reach secondary production target (consequently, a fission probability in the secondary target) is not at all a linear function of the incident charged particle energy. Furthermore, during the fission, induced by more energetic neutrons, more secondary neutrons will be emitted, and these will result in additional secondary fissions in the thick production target. Clearly, this secondary effect was not taken into account in [26], where the thin target yields were investigated.

In brief, a compromise of the two conflicting requirements: higher energies of

primary projectiles and lower energies of emitted neutrons as discussed above, has to be found. We choose a primary deuteron beam and a light metal target-converter resulting in an efficient source of high energy (approximately half energy of the incident deuteron) and forward peaked neutrons [21]. In this way we can easily look for an optimum energy of the incident projectile to produce the best yields of the neutron-rich isotopes of interest in the secondary production target.

The simplified RIB production assembly consists of a beam stopping beryllium cylinder (neutron source) and a uranium cylinder (production target) placed at 1cm distance from the first one as presented in Fig. 5. We note that at GANIL

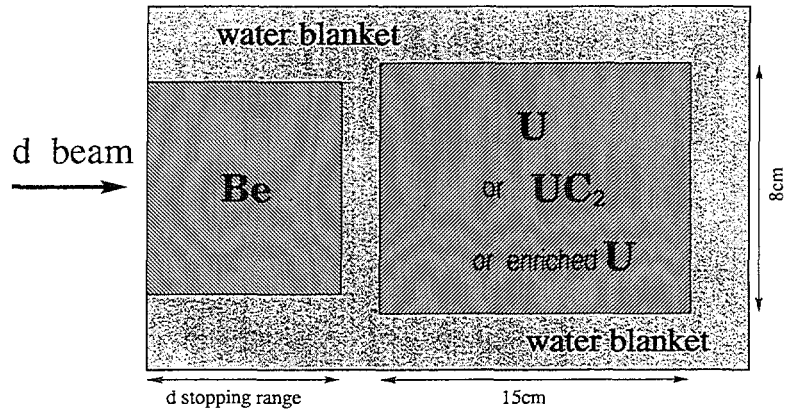

Fig. 5. A combined target assembly for neutron multiplication and isotope production with incident deuterons. The target units preserve a symmetry along the beam axis.

maximum energies are up to 100MeV/u. On the other hand, the validity of the simulations with LAHET for incident particle energies lower than 50MeV is more than questionable. Therefore, we limit our calculations to the incident deuteron energies E_d=50MeV, 100MeV, and 200MeV and change the length of the stopping beryllium target accordingly, i.e. l=1cm, 3cm, and 10cm. In order to minimise the neutron loss from the system, and at the same time to provide it with some cooling, the targets are surrounded by a cylindrical light water blanket (see Fig. 5). We note at this point that the LCS has been successfully benchmarked against fission isotopic yields in the energy range as above in [21].

We simulate a parallel deuteron beam which is uniformely distributed over an ellipse. Low energy neutrons ($E_n \leq$20MeV) are transported by HMCNP down to the thermal energies, and together with the tables of high energy spallation products, resulting from the LCS, are employed by the CINDER'90 code to calculate the final yields of the isotope production in the full range of neutron energies. We note that

in Ref. [21], where similar simulations have been made, the fission products from the fissions induced by low energy neutrons were not taken into account.

Neutron production in the beryllium target increases as a function of deuteron energy very sharply, i.e. a factor of 2 (or 4) increase in energy corresponds to a factor of 4 (or 10) increase in total neutron yield [21], and essentially to the increase of the range in the material. In this energy region, the beam intensity could not compensate neutron production at lower energies but at the same beam power. Therefore, the highest 200MeV energy is suggested. In the secondary target neutron production is proportional to the number of neutrons in the primary one; approximately 35-45% of all neutrons produced in the beryllium cross the front surface of the secondary target, where neutrons are further multiplied by (n,xn) and (n,f) reactions. The energy spectrum of incoming neutrons is again very important in this process; more fissions and more (n,xn) reactions will occur for more energetic neutrons (see Ref. [21] for more detailed analysis).

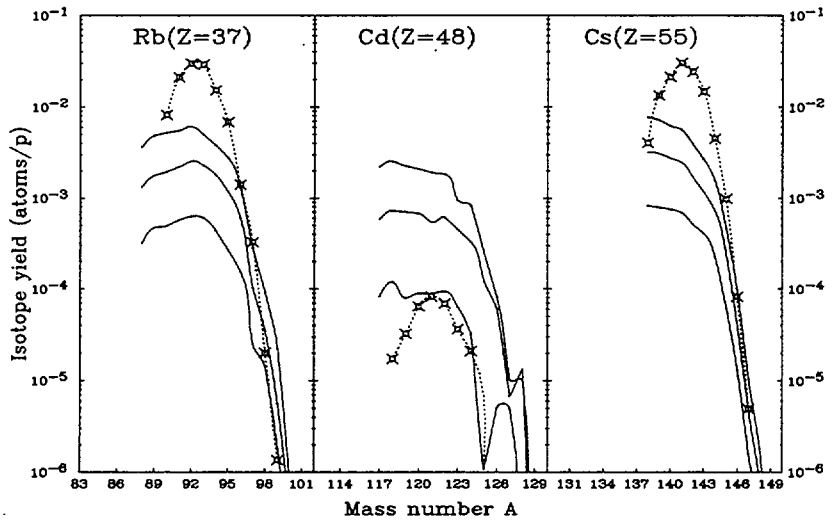

Fig. 6. Isotopic distributions of the in-target production of Rb, Cd and Cs in the systems of 200MeV, 100MeV and 50MeV d+Be → xn+U (solid curves from top-to-bottom in atoms per deuteron) (also see Fig. 5), and n_{th}+^{235}U (dotted curves in atoms per neutron/cm^2) as from [13].

In the fission of ^{238}U by reactor neutrons the mass distribution of fission products contains two peaks located at A=85-105 and A=125-150 [25]. In between these two peaks at mass A=105-125 the distribution has its local minimum. For a more detailed examination of isotope production in uranium by neutrons originating from the primary beryllium target we have chosen Rb (Z=37), Cd (Z=48) and Cs (Z=55)

isotopes located within three regions of the mass distribution of fission products as mentioned above.

The results with the ^{238}U production target and three different incident energies of deuterons are shown in Fig. 6, where isotope yields are normalised per incident deuteron. As expected, higher incident energies resulted in slightly broader isotope distributions (compare the curves with 50MeV and 200MeV deuterons, in particular). At the same time, at the very peaks of the distributions, increase in incident energy from 50MeV to 100MeV (to 200MeV) increased the isotope production by a factor of 4 (or 8). On the neutron-rich (or deficient) side these differences are similar if extrapolated from presently calculated values. From the above results the following conclusions can be made: E_d=100MeV seems to be an optimum incident energy in the RIB production target considered (see Fig. 5). Increase in energy from 100MeV up to 200MeV gave a similar increase in isotope production. This also could be achieved with 100MeV deuterons instead of 200MeV but with 2 times higher primary beam current, i.e. at the same beam power. Contrary, increase in energy from 50MeV up to 100MeV resulted in higher isotope production by a factor of 4, what could not be compensated at the same primary beam power, say for 50MeV deuterons with their beam intensity $2 \cdot I_o$ versus 100MeV deuterons with intensity I_o.

For comparison in Fig. 6 we also included isotope production distributions (dotted curves) from thermal neutron induced fissions in 1g of the uranium ^{235}U [13]. The isotope rates are normalised per incident neutron per cm^2 in this case. Near the peaks of the mass distribution of fission products, the n_{th}+^{235}U reactions give higher yields by 1 order of magnitude. However, fission yields from high energy neutrons resulted in broader isotope distributions, what makes these two different methods equally efficient on the neutron-rich and/or neutron-deficient of the distributions. In addition, in the mass region A=105-125, where fission products from thermal neutron induced fissions exhibit their local minimum, high energy neutrons give higher fission yields by a factor of 10-20 (compare curves for Cd isotope distribution in Fig. 6). More straightforward comparison of the two different methods discussed above is presented in Fig. 7, where one can easily see advantages/disadvantages these methods contain.

In order to compare the above proposed method for isotope production with the ones at already existing or planned experimental facilities in Europe, the relevant information provided in Table 1 is necessary.

The final RIB intensity I will depend on a number of parameters determined by the following expression:

$$I = I_o \cdot \sigma \cdot N \cdot \epsilon. \quad (1)$$

Here I_o stands for the incident beam intensity, σ is the production cross section of the particular radioactive isotope in the particular nuclear reaction, N is the thickness of the production target, and $\epsilon = \epsilon_1 \cdot \epsilon_2 \cdot \epsilon_3$ is the final efficiency factor defined by the product release and transfer efficiency ϵ_1, the ion-source efficiency ϵ_2, and the delay transfer efficiency ϵ_3 due to radioactive decay losses.

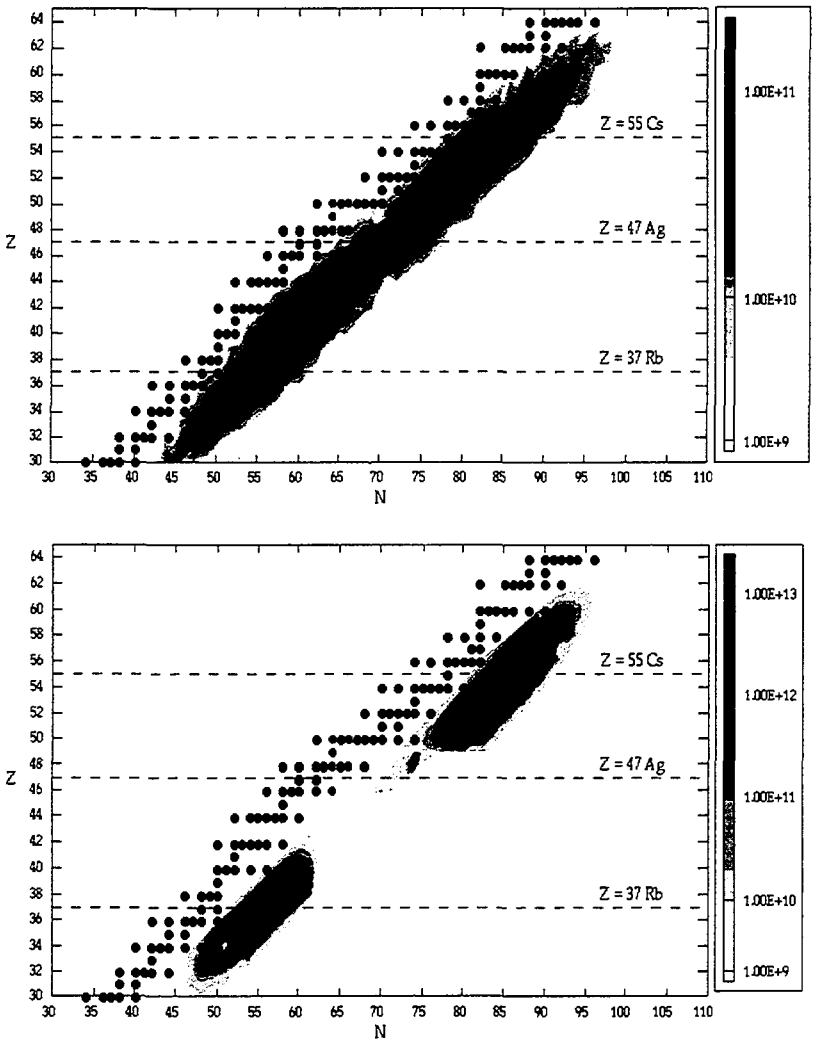

Fig. 7. Comparison of *in-target* fission yields in the case of 200MeV d+Be→xn+^{238}U [21] normalised for 1.9*10^{14}(d/s) (upper part) versus n_{th}+^{235}U as from [13] normalised for 1.9*10^{14}(n/s cm^2) (lower part). Black dots represent stable nuclei.

Table 1. Primary beam and target characteristics in some of the European RIB facilities in operation, under construction or proposed [24].

Project	Incident beam energy, particle	Target thickness (g/cm^2), element	Intensity $p\,\mu A$
ISOLDE (Geneve)	1GeV, protons	110, ^{238}U	3
GANIL (Caen)	100MeV/u, ^{12}C	5, ^{238}U	8
PIAFE (Grenoble)	thermal, neutrons	1, ^{235}U	$10^{14}/s\,cm^2$
SPIRAL-2 (Caen)	100MeV/u, deuterons	19, Be + 284, ^{238}U	30

In Table 2 we present projected *in-target* isotope production, i.e. a product of $I_o \cdot \sigma \cdot N$ as from Eq. 1, normalised to a primary beam intensity of one particle μA. We note, that these are estimations of *in-target* isotope production, and the final beam intensities may be reduced considerably (1-3 orders of magnitude) if the total efficiency ϵ of the ion-source is taken into account. We refer the reader to the Ref. [24], where more detailed analysis on this subject is given and where some of the ϵ values are given explicitly for different beam-target-isotope combinations. It should be also noted that an intensity of one particle μA for some primary beams is a high intensity whereas other particles may be availabe and usable in orders of magnitude higher intensities (see Table 1). Therefore, it is also very important to set realistic limits of the intensities of the primary beam currents.

In brief, as it is seen from Table 2, both ISOLDE and SPIRAL-2 *in-target* isotope production rates (in atoms per sμAp) are very similar, while present GANIL fragmentation technique gives smaller values by a factor of 2-10. In the case of the PIAFE project, the isotope production is smaller/higher by 1 order of magnitude depending on the atomic mass A of the fission products. (Also see Table 1 for the relevant information.)

If low density powders of UC_x are used in order to decrease the release time of isotopes, the corresponding yields have to be corrected by the ratio of the mean density [21], that is typically 1-2g/cm^3 for UC_x powders [27], over the corresponding density used in our calculations, i.e. $\sim$20g/cm^3 for ^{238}U. In addition, the fact, that the UC_x system apparently moderates faster the neutron spectrum to below the threshold energy of ^{238}U fission, and/or effectively scatters neutrons out of the system, has to be taken into account.

The use of highly enriched uranium for production of isotopes seems to be an interesting possibility too. In this context we investigated a subcritical secondary target consisting of 20% ^{238}U and 80% ^{235}U with its averaged density ρ=18.01g/cm^3. Criticality calculation with the MCNP code [17] resulted in an effective neutron multiplication coefficient k_{eff} $\sim$0.9 to be compared to k_{eff} $\sim$0.1 in the case of a pure ^{238}U cylinder with the same geometry setup. In this particular case, 70 times

Table 2. Estimate of projected *in-target* isotope production of RIB (the numbers for ISOLDE, GANIL and PIAFE facilities are taken from [24]). The lists of beam intensities are normalised to a primary beam intensity of one particle μA, except for the thermal neutron based PIAFE facility for which neutron flux densities of $6.25*10^{12}$ n/ s cm^2 have been considered. See Table 1 and Ref. [24] for details concerning the primary beams, incident particles, different target geometries and materials in the case of different experimental facilities.

Beam	ISOLDE at./sμA p	GANIL at./sμA p	PIAFE (see caption)	SPIRAL-2 at./sμA p
$^{78}_{30}$Zn	$2.3*10^8$	$3.5*10^7$	$3.8*10^8$	$4.5*10^8$
$^{91}_{36}$Kr	$4.1*10^9$	$5.8*10^8$	$2.7*10^{11}$	$2.4*10^{10}$
$^{94}_{36}$Kr	$1.7*10^8$	$4.9*10^7$	$8.8*10^9$	$4.9*10^9$
$^{97}_{37}$Rb	$8.7*10^8$	$4.6*10^8$	$4.6*10^9$	$1.8*10^9$
$^{132}_{50}$Sn	$1.5*10^8$	$2.6*10^7$	$5.4*10^{10}$	$9.3*10^9$
$^{142}_{54}$Xe	$1.3*10^8$	$2.3*10^7$	$4.1*10^{10}$	$8.0*10^9$
$^{144}_{54}$Xe	$2.7*10^6$	$4.8*10^5$	$7.5*10^8$	$5.6*10^8$
$^{144}_{55}$Cs	$2.2*10^{10}$	$3.9*10^9$	$3.4*10^{10}$	$8.9*10^9$

more fissions were obtained if compared with the target without ^{235}U [11]. Here we remind that the number of fissions at the first approximation

$$N_{fiss} \sim \frac{k_{eff}}{1 - k_{eff}}. \tag{2}$$

Consequently, the ratio of a number of fissions N_{fiss}(80% ^{235}U)/N_{fiss}(^{238}U)$\sim$80. A similar factor would result in the increase of the isotope production yields near the peaks of the fission products; even though all distributions would slightly be moved to the neutron deficient side (simply because $\frac{N}{Z}(^{235}\text{U}) < \frac{N}{Z}(^{238}\text{U})$). Such a target assembly, if considered, would allow to take advantages both of the thermal and high energy neutron induced fissions resulting in fission yields of the order of magnitude of 0.1 (atoms/d), i.e. even higher than in the case of the PIAFE project [13].

5. Energy amplification: protons or deuterons?

In a charged particle induced cascade one can distinguish two qualitative physical regimes: a) a spallation driven, high energy phase and b) a neutron driven, fission dominated regime. Neutrons from the first phase are acting as a "source" for the second phase, in which they gradually loose energy by collisions and are multiplied by (n,f) and (n,xn) reactions. Depending on the final aim, one must choose very carefully the target materials for both of these physical regimes. In this Chapter we

would like to develop in more detail the idea proposed already in 1952 during the measurements of neutron yields by bombardment of target assemblies with proton and deuterons beams. At that time two significant conclusions were reached [12]:

1. "In direct bombardment of (30cm) targets of uranium the yield in terms of neutrons per incident beam particle was 25% to 30% greater for deuterons than for protons of the same energy."

2. "In the case of deuteron bombardment, the insertion of a one-range thickness of lithium or beryllium (primary target) in front of the uranium block (secondary target) resulted in nearly the same neutron yield as bombarding uranium directly..."

Encouraged by these findings and motivated by those we pointed out in the previous Chapters, a simplified subcritical target assembly for neutron multiplication and energy production by proton and deuteron induced reactions was taken as a test case (see Fig. 8) [11]. Two different combinations were considered: a)

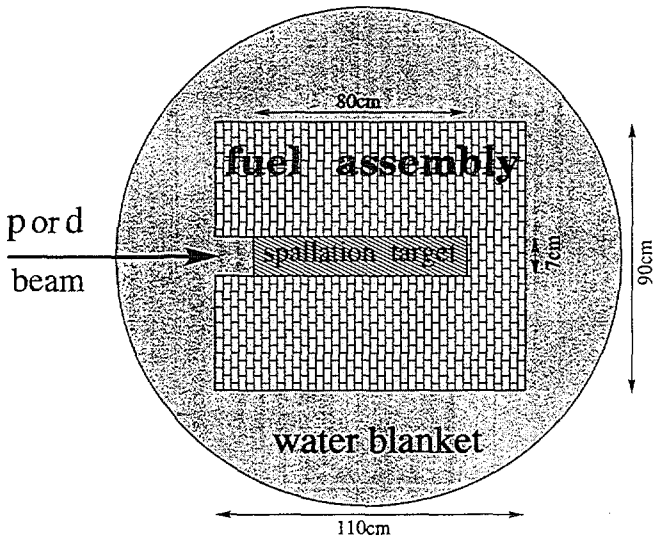

Fig. 8. A simplified subcritical (with k$\sim$0.9$\ll$1.0) target assembly for neutron multiplication and energy production with incident protons or deuterons. The target units preserve a symmetry along the beam axis.

beryllium spallation target placed inside the fuel assembly ("Be+fuel" hereafter), and b) uranium spallation target placed inside the fuel assembly ("U+fuel" hereafter). For simplicity a homogeneous water and uranium mixture was used as a fuel. The device is surrounded by a spherical water blanket, acting as a "reflector". We note that our simplified "reactor" can serve as a good approximation (as long as its geometry and materials are concerned) of a subcritical arrangement made of natural uranium rods (0.71% ^{235}U) and water moderator as described in [28], where

a measured effective neutron multiplication coefficient k=0.895±0.010 was reported [28]. We performed the criticality calculations with the MCNP code [17] by simulating a point-like neutron source placed in the middle of the spallation target [11]. With this configuration k=0.897 was obtained. By replacing the uranium spallation target with a beryllium bar in the same fuel assembly only a small increase in k value (of the order of 0.5%) was observed.

In addition to the total neutron yield normalised per incident beam particle, the total number of fissions N_{fiss} which took place in the fuel assembly was calculated [11]. After each successive fission in ^{238}U or ^{235}U approximately 181MeV energy becomes available according to their fission Q-values. Therefore, the energy gain $G(N_{fiss})$, i.e. the ratio of the energy produced in the device to the energy delivered by the beam, can be estimated by a very simple relation

$$G(N_{fiss}) = \frac{181\, N_{fiss}}{E_{beam}} \tag{3}$$

whith E_{beam} given in (MeV).

The results for the neutron production in such a subcritical "reactor" (see Fig. 8) in the case of the "U+fuel" target assembly just confirm the estimations already discussed above; protons (compared to deuterons) are almost equally efficient in neutron production at the same total incident energy if one chooses heavy metal target as Pb, Th or U for a spallation target. The difference depends on incident energy, chosen target material and its geometry, and ranges from 5% to 15% in favour of deuterons. Only a small difference was found for a number of fissions N_{fiss} in the fuel assembly as well, what results in nearly the same energy gain factor given by $G(N_{fiss})$, i.e. up to 10% higher for deuterons.

However, the "Be+fuel" target assembly gives much higher neutron yields for deuterons as incident projectiles. In the case of deuterons, we obtained nearly the same neutron multiplicities as for "U+fuel" assembly, in agreement with the measurements back in 1952 [12]. In the case of protons, neutron production is sharply decreased if compared to the one obtained bombarding the "U+fuel" system. Moreover, the "Be+fuel" target combination with deuterons results in a faster increase of the number of fissions N_{fiss} (and in the energy gain factor $G(N_{fiss}) \sim N_{fiss}$ following Eq. 3), as compared to the protons bombarding the "U+fuel" device. The reason for this difference is the following: as was already discussed above, neutrons originating from the light metal spallation target are much more energetic; hence, their multiplication in the fissile material results in a higher number of fissions N_{fiss} (and energy gain $G(N_{fiss})$) per incident particle until the optimum energy is reached.

In Fig. 9 we summarise the discussion above by plotting the calculated energy gain $G(N_{fiss})$ as a function of the incident beam energy and two different spallation targets ("Be" or "U") inside the same fuel assembly "fuel" (uranium and water mixture) for protons "p" and deuterons "d" (also see Fig. 8). In Fig. 9 we also add the experimental points (with error bars) from [28], which in our notation should be compared to the "p on U+fuel" solid curve. Inspite of the simplifications

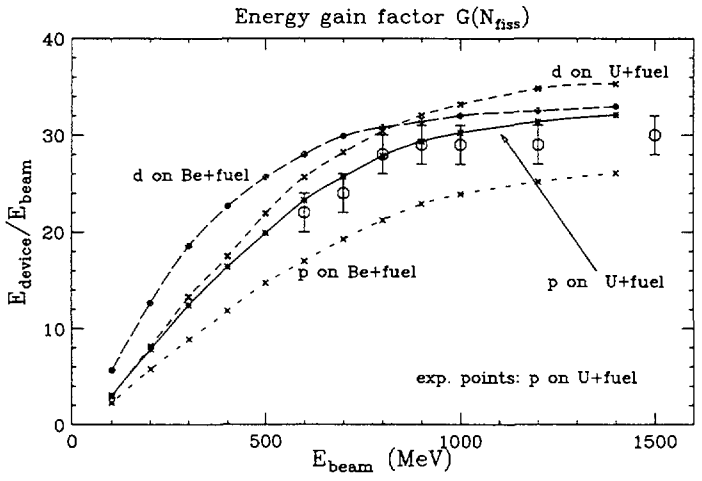

Fig. 9. Calculated [11] and measured. [28] average energy gain, i.e. the ratio of the energy produced by fissions in the device to the energy delivered by the beam, for proton and deuteron induced reactions on different spallation targets (Be or U) inside the same fuel assembly as a function of total incident energy.

we made in the geometry assumptions, we got a reasonable agreement with the experimental data; although in our calculations no neutron loss in the construction materials was taken into account. In addition, our predicted values for deuterons (see "d on Be+fuel" long-dashed curve) suggest that a practical energy amplifier could therefore be operated with deuteron beam energies of the order of 400MeV-800MeV, i.e. at lower incident energies by 400MeV than suggested in [28] for proton beam, and still give a comparable energy gain factor.

There might be more advantages of the light metal over heavy metal primary targets. In the case of light metal spallation target + fuel assembly, the heat will be distributed over a greater depth, and much of the beam power is carried forward into a secondary target by the high-energy neutrons. These neutrons penetrate the uranium fuel assembly with much better efficiency having about a 10cm mean free path for interaction. Therefore, the fuel burnup should be more homogeneous if compared to the case when charged particles are stopped in the fuel assembly itself.

6. Conclusions

We have tried to elucidate the question if proton or deuteron induced reactions are more efficient in neutron production. The complete optimisation of the neutron production efficiency involves three major parameters of interest: the energy spec-

tra of neutrons, the angular distributions of neutrons, and the averaged neutron multiplicities. Each of these parameters was found to be a function of a chosen projectile, its total incident energy and a chosen target material, what makes our initial task even more complicated.

(a) We estimated that neutron production by deuterons, if compared to proton induced reactions, is higher up to 250%, 150% and 10% for light, intermediate and heavy metal targets respectively. A combination of deuterons with a light target material gives the hardest neutron spectrum. The most isotropic angular distribution of neutrons is obtained in the p+U reaction, while the d+Be reaction resulted in the most forward peaked neutrons.

Consequently, what we have learned from the studies on neutron production (a) has become the essential part in the applications for RIB production via neutron induced fissions (b) as well as for accelerator-driven hybrid reactors (c).

(b) The SPIRAL Phase-II (GANIL) RIBs are neutron-rich nuclei in the mass region $75 \leq A \leq 160$. In order to produce them, the stopping target-converter (Be) interacting with intermediate energy deuterons was chosen and served as an efficient and forward peaked source of energetic neutrons to induce fissions in the secondary isotope-production target (U). It was found that in the energy range from 50MeV to 100MeV of the incident deuterons both the neutron and isotope production increases with beam energy for a constant beam power. For this reason, 100MeV deuterons are suggested, and further increase in primary beam energy for a target combination considered is not worth while. In the case of the pure ^{238}U secondary target, 80% of the incident beam power is deposited in the primary Be target, while the energy dissipated in the secondary U target is mostly due to the energy released by the fission process, i.e. the heat dissipation issue is solved automatically in the production target. Therefore, for the same power dissipated in the target, neutron fluxes can be one order of magnitude higher than the charged particle currents. Even with 10kW deuteron beam at 100MeV (compatible with the existing characteristics of GANIL) one could expect a 2-3 orders of magnitude increase in the final secondary beam intensity for some isotopes estimated from present fragmentation of the target and/or the heavy ion beam.

(c) The observed differences (both quantitave and qualitative) in neutron production from proton and deuteron induced reactions might be also very important in further investigations of the spallation target (ligh or heavy metal) within subcritical hybrid systems. In this case four possible combinations were considered: protons or deuterons bombarding the U or Be spallation target placed inside the same fissionable fuel assembly. We found that the "U+fuel" device gives 5-10% higher neutron yield per incident particle for deuterons than for protons at the same total energy. In the case of deuterons, the "Be+fuel" target assembly results in nearly the same neutron yield as for the "U+fuel" one. Now the heat is distributed over a much greater depth since more energetic neutrons are produced in Be spallation target. It was also predicted that the optimum energy gain in the modelled hybrid system may be reached at lower incident energies if deuterons are used instead of protons and a light metal target instead of a heavy one is employed as a spallation target

("d on Be+fuel" case). This lower energy should result in higher beam intensities, lower costs of the system and perhaps facilitate radioprotection problems.

The present conclusions **(a)**, **(b)**, and **(c)** will hold, to our opinion, qualitatively for other configurations; however, one always must take into account the precise device for a realistic optimisation. In addition, the findings reported here should be confirmed by new experimental data.

Acknowledgement

We would like to thank J.A. Nolen and A.C.C. Villari for fruitful discussions and comments at different stages of this manuscript. We also wish to express our appreciation to R.E. Prael (LANL) and W.B. Wilson (LANL) for providing us with the LAHET Code System and CINDER'90 codes respectively, and the Radiation Shielding Information Center (ORNL) for providing us with the MCNP code through the NEA Data Bank.

References

1. R. Serber, *Phys. Rev.* **72** (1947) 1114.
2. G.S. Bauer, 2nd Int. Conf. on Accelerator Driven Transmutation Technologies, Kalmar, Sweden, June 3-7 1996; also see at "http://www.psi.ch/".
3. *European Spallation Source (ESS) - a Next Generation Neutron Source for Europe*, available at "http://www.isis.rl.ac.uk/ESS/".
4. *Spallation Neutron Source (SNS) Status Report*, Oak Ridge National Laboratory, USA, available at "http://www.ornl.gov/sns/".
5. J.C. Browne *et al.*, 2nd Int. Conf. on Accelerator Driven Transmutation Technologies, Kalmar, Sweden, June 3-7 1996; also see at "http://public.lanl.gov/apt/".
6. H. Nifenecker, S. David, J.M.Loiseaux, A. Giorni, "Hybrid Nuclear Reactors", Institut des Sciences Nucléaires de Grenoble (ISN) **ISN 99.04**, (January 1999), submitted to *Progress in Particle and Nuclear Physics* at the request of the editor.
7. C.D. Bowman *et al.*, *Nucl. Instr. & Meth.* **A 320** (1992) 336.
8. C. Rubbia *et al.*, "Conceptual design of a fast neutron operated high power energy amplifier", *preprint* **CERN/AT/95-44** (ET) (1995).
9. T. Mukaiyama *et al.*, "Conceptual study of actinide burner reactors", International Reactor Physics Conference, Jackson Hole, WY (USA), 18-22 September 1988.
10. W.S. Park *et al.* "HYPER (HYbrid Power Extraction Reactor); a system for clean nuclear energy", July 1998 submitted to *Nuclear Science and Engineering*; W.S. Park, private communication.
11. D. Ridikas and W. Mittig, *Nucl. Instr. & Meth.* **A 418** (1998) 449; *GANIL preprint* **P 97 19**, GANIL, Caen (May 1997), available from CERN Library Catalogue at "http://alice.cern.ch/"
12. Status of the MTA process, *report* **LRL-102**, Livermore Research Laboratory

(February 1954); C.M. Van Atta, "A brief history of the MTA project", unpublished.
13. PIAFE Collaboration, "Piafe Project: Physics Case", SARA/ISN, Institute des Sciences Nucléaires de Grenoble (June 1994).
14. J.A. Nolen, Proceedings of the 3rd Int. Conf. on RNB, Gif-sur-Yvette, France, 24-27 May 1993, Ed. D.J. Morrissey, Editions Frontiers (1993) 111; Concept for Advanced Exotic Beam Facility Based on ATLAS, Argonne National Laboratory (February 1995); J.A. Nolen, private communication.
15. "R&D for the SPIRAL Phase-II: neutron-rich beams in high charge-states made by Deuterons", the EU contract ERB4062PL975009, April 1998 - May 2001; more information available at "http://www.ganil.fr/spiral2/".
16. R.E. Prael and H. Lichtenstein, "User Guide to LCS: The LAHET Code System," Los Alamos National Laboratory *report* **LA-UR-89-3014** (September 1989); R.E. Prael, private communication.
17. Group X-6, "A General Monte Carlo Code for Neutron and Photon Transport", LA-7396-M, Los Alamos National Laboratory (April 1981).
18. M. Blann, H. Gruppelar, P. Nagel, and J. Rodens, *International Code Comparison for Intermediate Energy Nuclear Data*, NEA OECD, Paris (1994); R. Michel and P. Nagel, *International Codes and Model Intercomparison for Intermediate Energy Activation Yields*, NSC/DOC(97)-1, OECD, Paris (1997).
19. D. Ridikas, W. Mittig and J.A. Tostevin *Phys. Rev.* **C 59** (1999) 1555; *GANIL preprint* **P 98 28**, GANIL, Caen (September 1998), available from CERN Library Catalogue at "http://alice.cern.ch/".
20. W.B. Wilson, T.R. England and K.A. Van Riper, "Status of CINDER'90 Codes and Data", Los Alamos National Laboratory *preprint* **LA-UR-99-361** (1999), submitted to Proc. of 4th Workshop on Simulating Accelerator Radiation Environments, September 13-16, 1998, Knoxville, Tennessee, USA; W.B. Wilson, private communication.
21. D. Ridikas and W. Mittig, Proceedings of the 2nd Int. Conf. on Exotic Nuclei and Atomic Masses (ENAM'98), Michigan, USA, 23-27 May 1998; AIP Conf. Series 455, Eds. B.M. Sherrill, D.J. Morrissey, and C.N. Davids, AIP, New York (1998) 1003; *GANIL preprint* **P 98 22**, GANIL, Caen (July 1998), available from CERN Library Catalogue at "http://alice.cern.ch/".
22. W. Mittig, *J. Phys G: Nucl. Part. Phys.* **24** (1998) 1331.
23. R. Leroy and A.C.C Villari, private communication.
24. H.L. Ravn *et al.*, *Nucl. Instr. & Meth.* **B 88** (1994) 441.
25. V.K. Rao *et al.*, *Phys. Rev.* **C 19** (1979) 1372.
26. I.C. Gomes, J.A. Nolen, "Influence of the incident particle energy on the fission product mass distribution", Proceedings of the 2nd Int. Topical Meeting on Nuclear Applications of Accelerator Technology, Gatlinburg, TN USA, September 20-23, 1998; J.A. Nolen, private communication.
27. A.E.Barzakh *et al.*, *Nucl. Instr. & Meth.* **B 126** (1997) 150; V.I. Tikhonov, private communication.
28. S. Andriamonje *et al.*,*Phys. Lett.* **B 348** (1995) 697.